

# Mössbauer studies of magnetic anisotropy for $\text{BaFe}_{12-2x}\text{Co}_x\text{Zr}_x\text{O}_{19}$

Z. W. Li,\* Linfeng Chen, and Xuesong Rao

*Temasek Laboratories, National University of Singapore, 10 Kent Ridge Crescent, Singapore, 119260*

C. K. Ong

*Center for Superconducting and Magnetic Materials and Department of Physics, National University of Singapore, 10 Kent Ridge Crescent, Singapore, 119260*

(Received 3 June 2002; published 10 February 2003)

The magnetic anisotropy of  $\text{BaFe}_{12-2x}\text{Co}_x\text{Zr}_x\text{O}_{19}$ , with  $x=0-1.2$  has been studied using Mössbauer spectra. Co and Zr ions are found to occupy the  $12k$  and  $2b$  sites preferentially. The quadrupole splittings suddenly decrease in magnitude and are even opposite in sign for the sample of  $x=1.2$ , as compared to other samples. The angle factor,  $b=A_{2,5}/A_{3,4}$ , are found to be 0.41 and 0.25 for  $x=0$  and 0.4, but 1.41 for  $x=1.2$ . These indicate that Co-Zr substitution can modify the anisotropy of  $\text{BaFe}_{12-2x}\text{Co}_x\text{Zr}_x\text{O}_{19}$ . A general formula of  $b$  is derived for nonfully aligned samples with the hexagonal structure by introducing the Gaussian-distribution of magnetic moments to a alignment direction. From the formula, the values of  $b$  are calculated to be  $4/3$  and zero for fully aligned samples with easy  $c$ -plane and easy  $c$ -axis anisotropies, respectively. In addition, the mean deviation of alignment is also obtained.

DOI: 10.1103/PhysRevB.67.054409

PACS number(s): 76.80.+y, 75.30.Gw, 75.50.Gg, 75.50.Ss

## I. INTRODUCTION

BaM ferrites have attracted much attention due to their extensive applications in industry, technology and daily life as permanent magnets, perpendicular recording media,<sup>1,2</sup> or electromagnetic wave absorption materials.<sup>3-5</sup> In all of these applications, a high saturation magnetization and Curie temperature are desired; however, coercivity is dependent on the various applications. Permanent magnets need a high coercivity; the recording media require an appropriate level of coercivity, while the absorption materials should essentially be a soft magnetic material. For BaM ferrites, coercivity is closely related to the magnetic anisotropy, which can be modified by substituting  $\text{Fe}^{3+}$  with other ions.

BaM ferrites have five Fe sites:  $4f_{VI}$ ,  $4f_{IV}$ ,  $2a$ ,  $2b$ , and  $12k$  sites. The distributions of substitution ions on the five sites can strongly influence magnetic properties, such as saturation magnetization and magnetic anisotropy.<sup>6-9</sup> It is known that Fe ions provide the largest positive contribution at the  $2b$  site, a relatively weak positive contribution at the  $4f_{VI}$ ,  $4f_{IV}$ , and  $2a$  sites,<sup>10,11</sup> and a negative contribution at the  $12k$  site.<sup>12</sup> Hence other ion substitutions for Fe ions could lead to an increase or decrease in the anisotropy field, and could even modify the anisotropy from an easy  $c$  axis to an easy  $c$  plane.<sup>13-15</sup>

Many techniques, such as torque, magnetization curve, and susceptibility, can be used to study the magnetic anisotropy. Mössbauer spectroscopy is one of the important tools. In Mössbauer spectra, the angle factor  $b$  is defined as the ratio of the intensities for the sum of the second and fifth lines to that of the third and fourth lines, i.e.,  $b=A_{2,5}/A_{3,4}$ , where  $A_{i,j}$  is the sum of the intensities for the  $i$ th and  $j$ th lines.  $b$  is given by

$$b = \frac{4(1 - \cos^2\beta)}{1 + \cos^2\beta}, \quad (1)$$

where  $\beta$  is the angle between the Fe magnetic moment and  $\gamma$ -ray propagation directions. Usually, for a sample with randomly oriented particles, the value of  $b$  is equal to 2. However, for an aligned sample, the value of  $b$  is zero when the sample has an easy  $c$ -axis anisotropy ( $\beta=0$ ) and the value is equal to 4 when magnetic moments are rotated into the  $c$  plane ( $\beta=\pi/2$ ). Based on Eq. (1), Li *et al.*<sup>16</sup> and Cadogan *et al.*<sup>17</sup> investigated the spin reorientation from an easy  $c$ -axis anisotropy at room temperature to an easy plane anisotropy at low temperature for aligned  $\text{DyFe}_{10}\text{Cr}_2$  and  $\text{DyFe}_{11}\text{Ti}$ .

In this paper, we report that the value of  $b$  is equal to  $4/3$  if an aligned sample with the hexagonal structure has a planar anisotropy. It is noted that Eq. (1) is valid only under the following conditions: (a) the sample has an easy  $c$ -axis anisotropy when it is aligned, and (b) The sample must be fully aligned. However, it is very difficult to prepare the fully aligned sample experimentally. Here we introduce the Gaussian distribution as a deviation function between the magnetic moments and alignment direction, and derive a general formula of  $b$  for nonfully aligned samples. Based on the formula,  $b=4/3$  is found for the easy  $c$ -plane anisotropy. To the best of our knowledge, these results have not been reported in theory or experiment previously. In addition, Mössbauer parameters ( $\delta$ ,  $\epsilon$ ,  $H_{hf}$ ), the site occupancy and the effect of these parameters on the magnetic properties are also discussed for  $\text{BaFe}_{12-2x}\text{Co}_x\text{Zr}_x\text{O}_{19}$ .

## II. EXPERIMENT

Samples of  $\text{BaFe}_{12-2x}\text{Co}_x\text{Zr}_x\text{O}_{19}$  with  $x=0, 0.2, 0.4, 0.6, 0.8$ , and  $1.2$ , were synthesized using conventional ceramic techniques. A mixture of  $\text{BaCO}_3$ ,  $\text{Fe}_2\text{O}_3$ ,  $\text{Co}_3\text{O}_4$ , and  $\text{ZrO}_2$  in the required ratio for BaM ferrite were presintered at  $1300^\circ\text{C}$  for 3 h, and subsequently crushed and ball milled. Finally, the powders were shaped and sintered in  $\text{O}_2$  at  $1200^\circ\text{C}$  for 6 h. Aligned samples were prepared by mixing fine powders of  $\text{BaFe}_{12-2x}\text{Co}_x\text{Zr}_x\text{O}_{19}$  with epoxy resin and

TABLE I. Lattice parameters  $a$  and  $c$ , special saturation magnetizations  $M_s$ , coercivity  $H_c$ , and anisotropy fields  $H_a$  for  $\text{BaFe}_{12-2x}\text{Co}_x\text{Zr}_x\text{O}_{19}$ .

$x$	$a$ (nm)	$c$ (nm)	$M_s$ (emu/g)	$H_c$ (Oe)	$H_a$ (kOe)
0	0.5898(2)	2.3226(6)	68.0(6)	2350(25)	17.2(5)
0.2	0.5900(2)	2.3229(7)	67.5(3)	1750(25)	14.0(1)
0.4	0.5899(1)	2.3233(10)	67.5(5)	510(20)	10.0(2)
0.6	0.5900(2)	2.3257(8)	61.0(3)	280(15)	8.2(2)
0.8	0.5901(1)	2.3268(5)	53.1(5)	10(10)	
1.2	0.5902(1)	2.3314(6)	33.5(2)	82(15)	5.0(3)

placing the mixture in an applied field of 4–8 kOe for Mössbauer experiments.

X-ray diffraction showed that all the  $\text{BaFe}_{12-2x}\text{Co}_x\text{Zr}_x\text{O}_{19}$  samples, with  $x=0-1.2$ , are single phase with hexagonal structure. The x-ray-diffraction patterns of the aligned samples show that samples with  $x=0$  and 0.4 have an easy  $c$ -axis anisotropy, while the sample with  $x=1.2$  has an easy  $c$ -plane anisotropy. The magnetic properties and lattice parameters are shown in Table I.

$^{57}\text{Fe}$  Mössbauer spectra were taken at room temperature using a conventional constant-acceleration spectrometer. The  $\gamma$ -ray source was  $^{57}\text{Co}$  in an Rh matrix. Calibration was performed using the spectrum of  $\alpha$ -Fe. Mössbauer spectrum of  $\text{BaFe}_{12-2x}\text{Co}_x\text{Zr}_x\text{O}_{19}$  with  $x=0$  was fitted by four sextets with Lorentzian line-shape, corresponding to the five different crystallographic sites  $4f_{VI}$ ,  $4f_{IV}+2a$ ,  $12k$ , and  $2b$ , respectively. For samples with  $x>0$ , the subspectrum on the  $12k$  site may be decomposed into two or three subcomponents,<sup>18</sup>  $12k_1$ , and  $12k_2$ , which correspond to various Co-Zr neighboring configurations at the  $12k$  site. Some constraints were used. The electrical-quadrupole interaction was treated as a perturbation on the magnetic-dipole interaction. The area ratios of the six absorption lines in each sextet were assumed to be 3:2:1:1:2:3 for nonaligned samples. For a given sextet, the six linewidths may be unequal because there may be various numbers of Co-Zr neighbors with different electric-quadrupole and magnetic-dipole interactions. Each line actually comprises unresolved overlapping patterns.

### III. RESULTS

#### A. Quadrupole splitting, isomer shift, and hyperfine field

Mössbauer spectra at room temperature for  $\text{BaFe}_{12-2x}\text{Co}_x\text{Zr}_x\text{O}_{19}$  together with fitted subspectra are shown in Fig. 1. The points in the figure are the experimental spectra and the solid lines represent the fitted curves.

The quadrupole splittings  $\langle \epsilon \rangle$  averaged over the  $4f_{VI}$ ,  $4f_{IV}$ ,  $2a$ , and  $12k$  sites and  $\epsilon_{2b}$  on the  $2b$  site, as a function of Co-Zr substitutions, are shown in Fig. 2(a). When  $x \leq 0.8$ , both  $\langle \epsilon \rangle$  and  $\epsilon_{2b}$  are considered as linear, to a good approximation. However, for the sample with  $x=1.2$ , there is sudden drop in magnitude for  $\langle \epsilon \rangle$  and  $\epsilon_{2b}$ , and there is a change in sign for  $\langle \epsilon \rangle$ . The values of  $\langle \epsilon \rangle$  and  $\epsilon_{2b}$  are

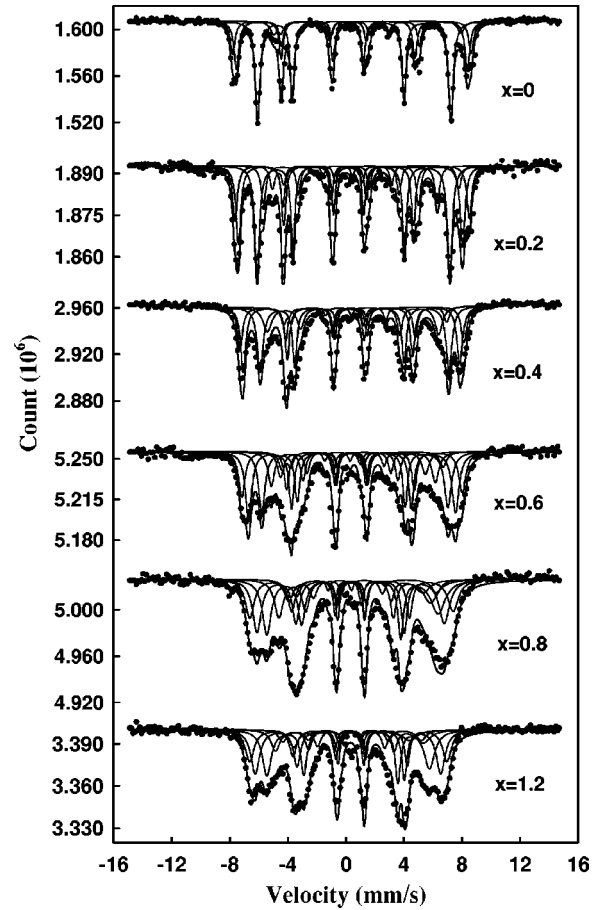


FIG. 1. Mössbauer spectra at room temperature for nonaligned  $\text{BaFe}_{12-2x}\text{Co}_x\text{Zr}_x\text{O}_{19}$  with the curves for the subspectra, obtained by a computer fit.

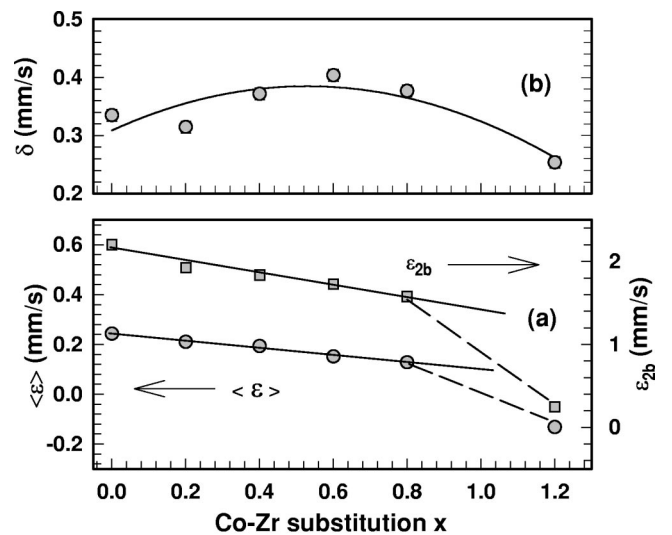


FIG. 2. Mössbauer parameters for  $\text{BaFe}_{12-2x}\text{Co}_x\text{Zr}_x\text{O}_{19}$ .  $\langle \delta \rangle$  is the average isomer shift over the five sites;  $\epsilon_{2b}$  and  $\langle \epsilon \rangle$  are the quadrupole splitting for the  $2b$  site and the average quadrupole splitting over the other four sites, respectively.

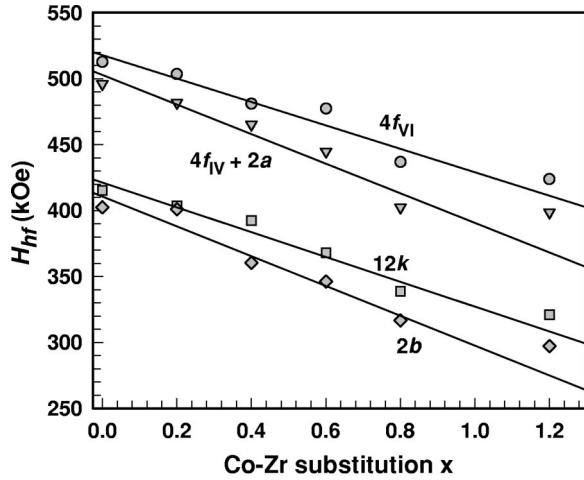


FIG. 3. Hyperfine field  $H_{hf}$  on the five sites for  $\text{BaFe}_{12-2x}\text{Co}_x\text{Zr}_x\text{O}_{19}$ .

–0.13 and 0.25 mm/s for the sample with  $x=1.2$ , respectively, as compared to 0.13 and 1.58 mm/s for  $x=0.8$ . It is well known that the quadrupole splitting  $\epsilon$  is related to the angle  $\theta$  between the directions of hyperfine fields and the principal axis of the electric-field gradient (EFG) by the equation

$$\epsilon = \frac{1}{4} e q Q (3 \cos^2 \theta - 1) \quad (2)$$

where  $Q$  is the nuclear quadrupole moment and  $q$  is the component of the EFG along the principal axis. When the magnetic moments of Fe atoms are either along the  $c$  axis or in the  $c$  plane, the quadrupole splitting will be significantly different in sign and/or in magnitude due to different  $\theta$ . Therefore, the dependence of  $\langle \epsilon \rangle$  and  $\epsilon_{2b}$  on the Co-Zr substitutions shows that the  $\text{BaFe}_{12-2x}\text{Co}_x\text{Zr}_x\text{O}_{19}$  samples have a change in magnetic anisotropy for  $x=1.2$ .

The dependence of the average isomer shift  $\langle \delta \rangle$  over the five sites on Co-Zr concentrations is shown in Fig. 2(b). With increasing Co-Zr ions, the isomer shifts first increase to a maximum at  $x=0.6$ , and then decrease. This feature is attributed to two opposite factors. One is the expansion of the cell volume, which leads to a decrease in the charge density at the nuclei. Hence there is an increase in the isomer shift. The other is a decrease in the average number of  $3d$  electrons with Co-Zr substitution. The decrease weakens the shielding effect of the  $3d$  electrons on the  $s$  electrons, which increases the charge density of the  $s$  electrons at the nuclei. As a result, the isomer shifts decrease.

Hyperfine fields on the five sites, as a function of the Co-Zr substitutions, are shown in Fig. 3. The hyperfine fields can be considered to be linear, to a good approximation for  $x=0-0.8$ . However, for the sample with  $x=1.2$ , the hyperfine fields deviate significantly from the lines, especially at the  $4f_{IV}+2a$  and  $2b$  sites. It appears that the deviation is associated with the change in anisotropy from the  $c$  axis to the  $c$  plane. It is known that the hyperfine field usually consists of the Fermi contact field, orbit field, dipole field, and supertransfer field. The decrease in the hyperfine fields with

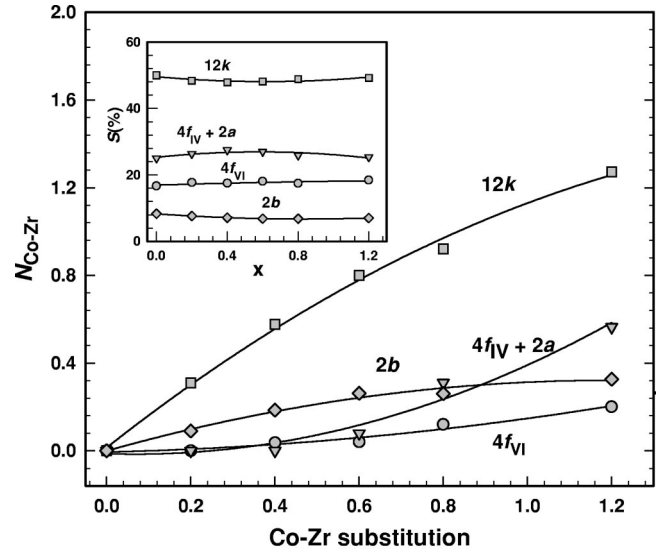


FIG. 4. Occupation numbers of Co-Zr ions on each site for  $\text{BaFe}_{12-2x}\text{Co}_x\text{Zr}_x\text{O}_{19}$ .

the Co-Zr substitutions is attributed to two factors. The first factor is the decrease in the Fermi contact field produced by the polarization of Fe ions. The Fermi contact field is dominant and is approximately proportional to the magnetic moment of Fe ions. The second factor is the decrease in the super-transfer field due to the magnetic ions (Fe and Co ions) surrounding a given Fe ion. These two fields are isotropic. However, the magnitude of the orbit and dipole fields are related to the direction of magnetic moments.<sup>19</sup> The orbit field can be ignored since the Fe ions are trivalent with spin of  $5/2$ . However, when the anisotropy is modified from the  $c$  axis to  $c$  plane, the dipole field will experience a sudden change in magnitude, leading to the deviation of the hyperfine fields at  $x=1.2$ . The jump in the hyperfine fields has also been observed at the Morin temperature for  $\alpha\text{-Fe}_2\text{O}_3$ ,<sup>20</sup> and at the spin-reorientation transition for R-Fe compounds.<sup>21</sup>

## B. Site occupation

A good fit was obtained for  $\text{BaFe}_{12}\text{O}_{19}$  using four subspectra with relative area ratios of 2:3:6:1 corresponding to the  $4f_{VI}$ ,  $2a+4f_{IV}$ ,  $12k$ , and  $2b$  sites. Therefore, it is reasonable to assume that the recoilless fractions on the five sites are the same. The relative areas  $S(i)$ , with  $i=1-4$ , of Mössbauer subspectrum for the five sites are shown in the insert of Fig. 4. From these areas, the occupation numbers  $N_{\text{Fe}}(i)$  and  $N_{\text{Co-Zr}}(i)$  of Fe and Zn-Zr ions on the  $i$ th site can be estimated based on the formulas

$$N_{\text{Fe}}(i) = C_{\text{Fe}} \frac{S(i)}{\sum_{i=1}^4 S(i)},$$

$$N_{\text{Co-Zr}}(i) = N(i) - N_{\text{Fe}}(i),$$

where  $C_{\text{Fe}}$  denotes the compositions of the Fe ions and  $N(i)$  is the total occupation number for the  $i$ th site. The results are shown in Fig. 4.

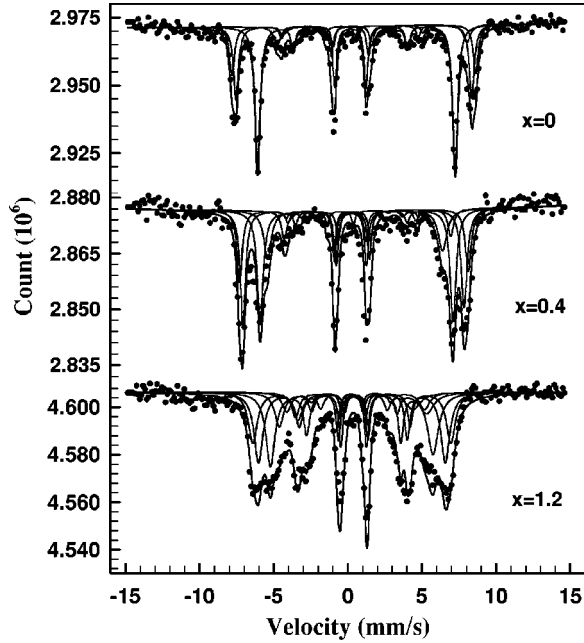


FIG. 5. Mössbauer spectra at room temperature for aligned  $\text{BaFe}_{12-2x}\text{Co}_x\text{Zr}_x\text{O}_{19}$  with the curves for the subspectra, obtained by a computer fit.

From Fig. 4, it is obvious that Co-Zr ions preferentially occupy the  $12k$  site in the whole range of  $x=0$  to 1.2 and the  $2b$  sites for  $x \leq 0.6$ . It appears that the  $4f_{VI}$  and  $4f_{IV} + 2a$  sites are not occupied by Co-Zr ions at  $x \leq 0.6$ . However, the occupancy on the  $4f_{IV} + 2a$  rapidly increases for  $x \geq 0.8$ . The site occupancies are similar to Co-Ti,<sup>7,9</sup> Co-Sn<sup>8</sup> and Co-Mo (Ref. 22) substitutions in BaM ferrites, but are different from the Zn-Zr substitution. For the Zn-Zr substituted BaM ferrites, the Zn-Zr ions preferentially occupy the  $4f_{VI}$  and  $2b$  sites, while the  $12k$  site is involved in the substitutions at  $x \geq 0.8$ . The  $4f_{IV}$  and  $2a$  sites seem not to be occupied by Zn-Zr ions for  $x=0-0.8$ .<sup>6</sup> Therefore, it is reasonable to deduce that the Co ions preferentially occupy the  $12k$  site and the Zr ions occupy the  $2b$  site for  $\text{BaFe}_{12-2x}\text{Co}_x\text{Zr}_x\text{O}_{19}$ .

It is known that the high magnetocrystalline anisotropy of BaM ferrites has its primary origin in  $\text{Fe}^{3+}$  on the trigonal bipyramidal site, i.e., the  $2b$  site,<sup>10,12</sup> which has large asymmetry. Therefore, the preference of Zr ions on the  $2b$  sites leads to a significant decrease in the anisotropy field for  $\text{BaFe}_{12-2x}\text{Co}_x\text{Zr}_x\text{O}_{19}$ . On the other hand,  $\text{Fe}^{3+}$  ions with up-spin are distributed on the  $2a$ ,  $12k$ , and  $2b$  sites and ions with down-spin are located on the  $4f_{VI}$  and  $4f_{IV}$  sites. The Co and Zr ions do not occupy the  $4f_{VI}$  and  $4f_{IV}$  site for  $x \leq 0.6$ . The moment of  $\text{Co}^{2+}$  ions are smaller than that of  $\text{Fe}^{3+}$  and the moment of Zr ions is zero. Consequently, the magnetizations decrease with Co-Zr substitution and the maximum in the magnetization is not observed at low Co-Zr substitution.

### C. Mössbauer spectra of aligned samples

The Mössbauer spectra and their fitted curves are shown in Fig. 5 for the aligned  $\text{BaFe}_{12-2x}\text{Co}_x\text{Zr}_x\text{O}_{19}$ . In fitting these Mössbauer spectra, all isomer shifts, quadrupole split-

TABLE II. Mössbauer parameters for the aligned  $\text{BaFe}_{12-2x}\text{Co}_x\text{Zr}_x\text{O}_{19}$  with  $x=0, 0.4$ , and 1.2.  $b$  is the angle factor,  $\sigma$  is the mean deviation based on Eqs. (14) and (15), and  $\beta$  is obtained from Eq. (1).

$x$	$b$	$\sigma$ (degree)	$\beta$	Anisotropy
0	0.41(15)	24.7(4.1)	25.5(3.1)	$c$ axis
0.4	0.25(9)	19.7(3.3)	20.1(2.4)	$c$ axis
1.2	1.41(12)	11.8(9.1)		$c$ plane

tings, hyperfine fields, linewidths and the area ratios of the subspectra were constrained to be the same as those for the non-aligned samples. However, the ratio of the six absorption lines in each sextet was assumed to be  $3:b:1:1:b:3$ , where the angle factor  $b$  is a fitted parameter. The fitted values of  $b$ , as shown in Table II, are 0.41, 0.25, and 1.41 for the samples of  $x=0, 0.4$ , and 1.2, respectively.

Here, two problems need to be resolved: (1) The value of  $b$ , as expected, is close to zero for  $x=0$  and 0.4 due to their easy  $c$ -axis anisotropies. However, for the sample with  $x=1.2$ , the value of  $b$  is about  $4/3$ . Why is  $b$  equal to  $4/3$ , and not equal to 4 or other values? (2) The values of  $b$  are not exactly equal to zero and  $4/3$  for the samples with easy  $c$  axis and easy  $c$ -plane anisotropies, respectively. This implies that the magnetic moments either deviate from the alignment direction or are distributed around the alignment direction. How to estimate the deviation? The two problems will be discussed in Sec. IV.

## IV. DISCUSSION

A sample with hexagonal structure is ground into very fine particles, which are considered to be single crystal. The particles are aligned in an applied magnetic field to make an aligned sample. The alignment field is perpendicular to the surface of the sample. Therefore, the directions of both the alignment field and the  $\gamma$ -ray propagation are along the  $z$  axis.

For a fully aligned sample with an easy  $c$ -axis anisotropy, the particles are aligned along the  $[001]$  direction in the demagnetized state. The direction of magnetic moments is given by

$$\mathbf{m}_{001} = \begin{pmatrix} 0 \\ 0 \\ 1 \end{pmatrix}. \quad (3)$$

When the sample has an easy-plane anisotropy, these particles are aligned along one of their  $a$  crystal axes,  $[100]$ ,  $[110]$  or  $[010]$  direction. In the demagnetized state, the directions of magnetic moments (or hyperfine field) are given by

$$\mathbf{m}_{100} = \begin{pmatrix} 0 \\ 3/2 \\ 1/2 \end{pmatrix} \quad \mathbf{m}_{110} = \begin{pmatrix} 0 \\ 0 \\ 1 \end{pmatrix} \quad \mathbf{m}_{010} = \begin{pmatrix} 0 \\ -3/2 \\ 1/2 \end{pmatrix}. \quad (4)$$

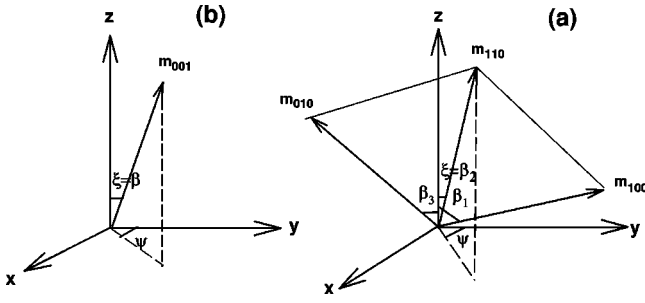


FIG. 6. Geometrical arrangements of magnetic moments  $\mathbf{m}$  and deviation angle  $\xi$  in  $x$ - $y$ - $z$  coordinates for (a) easy  $c$ -plane and (b) easy  $c$ -axis anisotropies, respectively. Aligned magnetic field and  $\gamma$ -ray propagation are along the  $z$  axis.

For a nonfully aligned sample, it is assumed that the  $[110]$  and  $[001]$  crystal axes deviate from the  $z$  axis by a small angle  $\xi$  for the easy  $c$ -plane and easy  $c$ -axis anisotropy, respectively, as shown in Figs. 6(a) and 6(b). The possible directions of the moments  $\mathbf{m}_i^*$  ( $i=[100], [110], [010]$  or  $[001]$ ) of all particles can be represented as a rotation of the moment  $\mathbf{m}_i$  as an angle  $\xi$  around the  $y$  axis, followed by an angle  $\psi$  around the  $z$  axis. Hence the rotation matrix  $R = R_z(\psi)R_y(\xi)$  is expressed as

$$R = \begin{pmatrix} \cos \xi \cos \psi & -\sin \psi & \sin \xi \cos \psi \\ \cos \xi \sin \psi & \cos \psi & \sin \xi \sin \psi \\ -\sin \xi & 0 & \cos \xi \end{pmatrix}. \quad (5)$$

Therefore, the directions of the moments  $\mathbf{m}_i^*$  in  $x$ - $y$ - $z$  coordinates are given by

$$\mathbf{m}_i^* = R\mathbf{m}_i, \quad (6)$$

and the angles  $\beta_i$  between the direction  $\mathbf{m}_i^*$  and the  $z$  axis (the direction of  $\gamma$ -ray propagation) are obtained from

$$\cos \beta_i = \mathbf{m}_i^* \bullet \mathbf{z}. \quad (7)$$

For the sample with the easy  $c$ -axis and  $c$ -plane anisotropies,  $\beta_i$  is given by

$$\cos \beta_{001} = \cos \xi \quad (8)$$

and

$$\begin{aligned} \cos \beta_{100} &= 1/2 \cos \xi, \\ \cos \beta_{110} &= \cos \xi, \\ \cos \beta_{010} &= 1/2 \cos \xi, \end{aligned} \quad (9)$$

respectively. On the other hand, the probability distribution of  $\xi$  is assumed to be Gaussian, viz.

$$P(\xi) = \frac{1}{\sqrt{2\pi}\sigma} \exp\left(-\frac{\xi^2}{2\sigma^2}\right), \quad (10)$$

where  $\sigma^2$  is the mean-square deviation.

The areas of the six absorption lines for a Mössbauer spectrum are related to the angle  $\beta_i$  by the relationships

$$\begin{aligned} A_{1,6} &= \int_{-\infty}^{\infty} P(\xi) \frac{3}{4} (1 + \cos^2 \beta_i) d\xi, \\ A_{2,5} &= \int_{-\infty}^{\infty} P(\xi) (1 - \cos^2 \beta_i) d\xi, \\ A_{3,4} &= \int_{-\infty}^{\infty} P(\xi) \frac{1}{4} (1 + \cos^2 \beta_i) d\xi, \end{aligned} \quad (11)$$

where  $A_{i,j}$  represents the relative absorption area of the  $i$  and  $j$  lines.

Substituting the expressions for  $\cos \beta_i$  in Eq. (8) or (9) into Eq. (11) and using approximations,  $\sin^2 \xi \approx \xi^2$  and  $\cos^2 \xi \approx 1 - \xi^2$  for small  $\xi$ , the angle factor  $b$  can be obtained as

$$b = \frac{\int_{-\infty}^{\infty} P(\xi) (1 - \cos^2 \beta_1) d\xi}{\int_{-\infty}^{\infty} P(\xi) \frac{1}{4} (1 + \cos^2 \beta_1) d\xi} = \frac{4\sigma^2}{2 - \sigma^2} \quad (12)$$

and

$$b = \frac{\sum_{i=1}^3 \int_{-\infty}^{\infty} P(\xi) (1 - \cos^2 \beta_i) d\xi}{\sum_{i=1}^3 \int_{-\infty}^{\infty} P(\xi) \frac{1}{4} (1 + \cos^2 \beta_i) d\xi} = \frac{4(1 + \sigma^2)}{3 - \sigma^2} \quad (13)$$

for the easy  $c$ -axis and  $c$ -plane anisotropies, respectively.

From the above analysis, two important results are obtained: (a) for the fully aligned sample with the  $c$ -axis anisotropy, the angle factor  $b$  is equal to zero, based on Eq. (12), and for the sample with the  $c$ -plane anisotropy,  $b = 4/3$ , as obtained from Eq. (13); and (b) for the non-fully aligned sample, the angles  $\xi$  have a distribution; the mean deviation  $\sigma$  can be calculated from Eqs. (12) and (13). The value of  $\sigma$  is given by

$$\sigma = \sqrt{\frac{2b}{4+b}}, \quad (14)$$

$$\sigma = \sqrt{\frac{|3b-4|}{4+b}}. \quad (15)$$

For the aligned samples with  $x=0$  and  $0.4$ , the values of  $b$  are  $0.41$  and  $0.25$ , respectively. Hence, the two samples have an easy  $c$ -axis anisotropy. On the other hand,  $b = 1.41$  implies that the sample with  $x = 1.2$  has a  $c$ -plane anisotropy. As it is very difficult to prepare fully aligned samples, the values of  $b$  are not exactly equal to zero or  $4/3$ , which means that the magnetic moments deviate from the alignment direction. The mean deviations are found to be  $24.7^\circ$ ,  $19.7^\circ$ , and  $11.8^\circ$  for the samples with  $x=0$ ,  $0.4$  and  $1.2$ , respectively, based on Eqs. (14) and (15). From Eq. (1) we can obtain the averaged angles  $\beta$  of  $25.5^\circ$  and  $20.1^\circ$  for the samples with  $x=0$  and  $0.4$ , respectively. The values obtained from the two methods are close. However, for the sample with the  $c$ -plane

anisotropy ( $x=1.2$ ),  $b=4/3$ , and the mean deviation  $\sigma$  can be obtained only from the method discussed here, viz Eqs. (13) and (15).

## V. CONCLUSIONS

In this paper, we found the following.

(1) For the aligned  $\text{BaFe}_{12-2x}\text{Co}_x\text{Zr}_x\text{O}_{19}$ , the angle factors  $b=A_{2,5}/A_{3,4}$  are 0.41 and 0.25 for  $x=0$  and 0.4, but are equal to 1.41 for  $x=1.2$ . A general formula for  $b$  is derived for nonfully aligned samples with the hexagonal structure by introducing the Gaussian-distribution of magnetic moments to the alignment direction. Based on the formula, we identify

that  $\text{BaFe}_{12-2x}\text{Co}_x\text{Zr}_x\text{O}_{19}$  has an easy  $c$ -axis anisotropy for the samples with  $x=0$  and 0.4, and an easy  $c$ -plane anisotropy for the sample with  $x=1.2$ . In addition, the mean deviations of alignment are also derived; they are  $24.7^\circ$ ,  $19.7^\circ$ , and  $11.8^\circ$  for  $x=0$ , 0.4, and 1.2, respectively.

(2) From the Mössbauer spectra, the quadrupole splittings have a sudden decrease in magnitude and in opposite sign for the sample with  $x=1.2$ , as compared to other samples. This implies that Co-Zr substitution modifies the anisotropy of  $\text{BaFe}_{12-2x}\text{Co}_x\text{Zr}_x\text{O}_{19}$ . The Co ions preferentially occupy the  $12k$  site and Zr ions the  $2b$  site. The occupancy of Zr ions on the  $2b$  site leads to a decrease in the anisotropy field.

\*Electronic address: tsllizw@nus.edu.sg

<sup>1</sup>D. E. Speliotis, IEEE Trans. Magn. **31**, 2877 (1995).

<sup>2</sup>T. Fujiwara, IEEE Trans. Magn. **21**, 1480 (1985).

<sup>3</sup>D. Autissier, A. Podembski, and C. Jacquiod, J. Phys. IV **7**, C1-409 (1997).

<sup>4</sup>Han-Shin Cho and Sung-Soo Kim, IEEE Trans. Magn. **35**, 3151 (1999).

<sup>5</sup>S. Sugimoto, S. Kondo, K. Okayama, H. Nakamura, D. Book, T. Kagotani, M. Homma, H. Ota, M. Kimura, and R. Sato, IEEE Trans. Magn. **35**, 3154 (1999).

<sup>6</sup>Z. W. Li, C. K. Ong, Z. Yang, F. L. Wei, X. Z. Zhou, J. H. Zhao, and A. H. Morrish, Phys. Rev. B **62**, 6530 (2000).

<sup>7</sup>X. Z. Zhou, A. H. Morrish, Z. Yang, H. X. Zeng, J. Appl. Phys. **75**, 5556 (1994).

<sup>8</sup>X. Z. Zhou, A. H. Morrish, Z. W. Li, and Y. K. Hong, IEEE Trans. Magn. **27**, 4654 (1991).

<sup>9</sup>A. R. Corradi, D. E. Speliotis, A. H. Morrish, Q. A. Pankhurst, X. Z. Zhou, G. Bottoni, D. Candolfo, A. Cecchetti, and F. Masoli, IEEE Trans. Magn. **24**, 2862 (1988).

<sup>10</sup>N. Fuchikami, J. Phys. Soc. Jpn. **34**, 760 (1965).

<sup>11</sup>G. Asti and S. Rinaldi, in *Magnetism and Magnetic Materials-1976*, edited by J. J. Becker and G. H. Lander, AIP Conf. Proc. No. 34 (AIP, New York, 1976), p. 214.

<sup>12</sup>Y. Xu, G. L. Yang, A. P. Chu, and H. R. Zhai, Phys. Status Solidi B **157**, 685 (1990).

<sup>13</sup>K. Haneda and H. Kojima, Jpn. J. Appl. Phys. **12**, 355 (1973).

<sup>14</sup>E. Brando, H. Vincent, O. Dubrinfaut, A. Fourier-Lamer, and R. Lebourgeois, J. Phys. IV **7**, C1-421 (1997).

<sup>15</sup>J. Kreisel, H. Vincent, F. Tasset, M. Pate, and J. P. Ganne, J. Magn. Magn. Mater. **224**, 17 (2001).

<sup>16</sup>Hong-Shuo Li, Bo-Ping Hu, and J. M. D. Coey, Hyperfine Interact. **45**, 233 (1989).

<sup>17</sup>J. M. Cadogan, D. H. Ryan, and J. B. Dunlop, Hyperfine Interact. **94**, 1951 (1994).

<sup>18</sup>G. Albanese, M. Carbuicchio, and G. Asti, J. Appl. Phys. **11**, 81 (1976); G. Albanese, A. Deriu, E. Lucchini, and G. Slokar, Appl. Phys. A: Solids Surf. **26**, 45 (1981).

<sup>19</sup>R. L. Streever, Phys. Rev. B **19**, 2704 (1979).

<sup>20</sup>F. van der Woude, Phys. Status Solidi **17**, 417 (1966).

<sup>21</sup>P. C. M. Gubbens, A. M. van der Kraan, T. H. Jacobs, and K. H. J. Buschow, J. Magn. Magn. Mater. **80**, 265 (1989); Hu Bo-Ping, Li Hong-shuo, Sun Hong, J. F. Lawler, and J. M. D. Coey, Solid State Commun. **76**, 587 (1990); P. C. M. Gubbens, A. A. Moolenaar, G. J. Boender, and A. M. van der Kraan, J. Magn. Magn. Mater. **97**, 69 (1991).

<sup>22</sup>D. G. Agresti, T. D. Shelfer, Y. K. Hong, and Y. J. Paig, IEEE Trans. Magn. **25**, 4069 (1989).